Iranian Journal of Science and Technology, Transactions of Civil Engineering
https://doi.org/10.1007/s40996-024-01573-9

RESEARCH PAPER

Enhancing Concrete Strength and Durability of Normal and High-Strength Concrete: Exploring Combined Effects of Optimized Silica Fume and Slag

Davood Mostofinejad[1] · Mohsen Nasrollahi[1] · Hadi Bahmani[1] · Zahra Zajshoor[1] · Morteza Sadeghi[1]

Received: 13 May 2024 / Accepted: 29 July 2024

Abstract
Using supplementary cementitious materials in concrete attracted significant attention worldwide due to environmental benefits and the potential for enhancing concrete's mechanical properties and durability. This study investigates the interaction effects of silica fume and ground granulated blast furnace slag on the behavior of normal and high-strength concrete regarding steel corrosion resistance, carbonation depth, and compressive strength. Fifty-two concrete specimens were prepared in four groups with different combinations of water-to-cementitious materials ratio (w/cm), slag content, and silica fume content and were tested. A method was employed to compare the corrosion initiation times of different concrete specimens. The results demonstrated that silica fume improves the concrete's resistance to steel corrosion by enhancing the cement matrix's density, strength, and durability. The specimen with a w/cm ratio of 0.3 containing 35% slag and 10% silica fume achieved a 33% reduction in carbonation depth and a compressive strength of 118 MPa, representing a 20% increase compared to the similar specimen without slag. Furthermore, the specimen with a w/cm ratio of 0.3 containing 35% slag and 15% silica fume exhibited a 44% increase in steel corrosion resistance compared to the similar specimen without silica fume. While optimizing the combined content of slag and silica fume, this study highlights that their individual effects are less significant than their combined effect when used as partial replacements for cement.

Keywords Durability · Slag; Silica fume · Carbonation depth · Steel corrosion · Chloride ion penetration

1 Introduction

The durability of concrete has long been a fundamental aspect of concrete technology, as it must endure the environmental conditions for which it is designed throughout its structural lifespan. When assessing the durability of concrete structures, particularly in corrosive environments, experts emphasize that resistance alone is insufficient. Concrete design must account for various environmental conditions (Kurtis and Mehta 1997). Concrete structures can encounter various issues during their service life due to external factors induced by the surrounding environment and internal factors that can compromise concrete durability. These factors generally fall into three categories: physical, such as freeze–thaw action; mechanical, like abrasion; and chemical, including sulfate attack and acid corrosion of reinforcements (Committee and C. of M. in Concrete 1975; Mehri et al. 2023). The alkaline environment of concrete fosters the formation of a temporary and unstable microscopic iron oxide layer on the metal surface, providing corrosion protection. However, as concrete's alkalinity decreases and ion attacks occur, this protective coating on the steel's surface deteriorates (Aitcin 1993). Carbonation is the most common mechanism responsible for reducing the alkalinity of concrete (Kurtis and Mehta 1997). Furthermore, the penetration of chloride ions into steel rebar surfaces leads to corrosion,

✉ Mohsen Nasrollahi
m.nasrollahi@cv.iut.ac.ir

Davood Mostofinejad
dmostofi@cc.iut.ac.ir

Hadi Bahmani
h.bahmani@cv.iut.ac.ir

Zahra Zajshoor
z.zajshoor@cv.iut.ac.ir

Morteza Sadeghi
sadeghimorteza789@gmail.com

[1] Department of Civil Engineering, Isfahan University of Technology (IUT), Isfahan 84156-83111, Iran

Published online: 10 August 2024

diminishing the durability of reinforced concrete structures (Kurtis and Mehta 1997). To address this, producing low-permeability concrete has gained attention to enhance its durability and corrosion resistance (Committee and C. of M. in Concrete 1975; Mehri et al. 2023; Aitcin 1993; Hooton 1993). Consequently, extensive research has been conducted to explore steel corrosion prevention methods, such as cathodic protection (Committee and C. of M. in Concrete 1975), corrosion inhibitors (Aitcin 1993), and epoxy coatings (Hooton 1993), but these methods are expensive and have limited effectiveness. Alternatively, supplementary cementitious materials, partially replacing Portland cement, hold promise for sustainable and adequate corrosion resistance improvement (Iravani 1996; Ozyildirim 1993). Notably, pozzolanic admixtures, like silica fume (SF), fly ash (FA), and granulated blast furnace slag (GBFS), are among the most commonly used supplementary cementitious materials to prepare dense and robust concrete (Pigeon et al. 1993; Bayasi and Zhou 1993; Pettersson and Sandberg 1997; Li et al. 1999).

The advent of new construction materials and techniques has made the production of high-performance concrete feasible, achieved by incorporating silica fume additives, superplasticizers, and low w/cm ratios, resulting in better compaction and viscosity. High-performance concrete exhibits low permeability, which plays a crucial role in minimizing the ingress of contaminants like chloride, carbon dioxide, and humidity, known to initiate corrosion (Bahmani and Mostofinejad 2023, 2022; Hajiaghamemar et al. 2022). Silica fume serves two critical roles in concrete. First, its pozzolanic properties lead to a chemical reaction with calcium hydroxide (CH) to generate additional hydrated calcium silicate (C-S–H), enhancing concrete strength. Second, due to its minute particle size, silica fume fills all the microscopic pores in the cement paste, reducing its permeability (Li et al. 1999; Scanton and Sherman 1996). Consequently, adding silica fume to the concrete mixture in appropriate proportions significantly decreases concrete permeability and corrosion rate while improving its strength and durability (Chuang and Huang 2013; Voo and Foster 2010; Wei and Song 2005; Mohd Faizal et al. 2015). Research suggests that incorporating 15% silica fume in concrete enhances its long-term corrosion resistance (Berke 1989). Increasing the silica fume content from 10 to 20% does not substantially increase corrosion resistance (Al-Saadoun and Al-Gahtani 1992). Incorporating 7% silica fume, 45% graded blast furnace slag, 35% fly ash, and 15% zeolite resulted in a threefold increase in electrical resistivity and a sevenfold decrease in corrosion rate (Ghanbari et al. 2023).

Granulated Blast Furnace Slag (GGBFS) significantly enhances the corrosion resistance of concrete by reducing porosity, refining pore structure, and decreasing chloride ion mobility, with 50% GGBFS providing resistance comparable to 10% silica fume (Song and Saraswathy 2006; Li and Roy 1986; Torll et al. 1995). As for corrosion resistance, up to 60% of GGBFS replacement is effective and significantly reduces chloride ion diffusion (Huang and Yang 1997). However, high GGBFS levels may increase carbonation, particularly in dry indoor environments, although moist conditions mitigate this effect (Osborne 1992). To balance these factors, limiting GGBFS content to 50% in carbonation-prone environments is recommended, ensuring optimal durability without compromising corrosion resistance (Song and Saraswathy 2006; Osborne 1992).

The utilization of silica fume and slag has gained significant attention not only for their ability to enhance concrete durability and strength but also for their environmental benefits and potential to reduce cement consumption. Consequently, this study undertakes a comprehensive investigation of these two SCMs as partial replacements for cement. Despite extensive research on concrete durability, a thorough understanding of how different slag and silica fume proportions influence overall durability still needs to be discovered. Identifying the optimal combination of these supplementary cementitious materials (SCMs) to enhance concrete's resistance to steel rebar corrosion is an ongoing endeavor.

This study delves into the impact of incorporating silica fume, slag, and their various combinations at different proportions and water-to-cement (w/c) ratios on critical durability factors, including steel corrosion, carbonation penetration, and compressive strength. While previous studies have explored the individual effects of these SCMs, their combined influence and the optimal proportions for enhancing concrete durability still need to be discovered.

The overarching objective of this investigation is to unravel the intricate interplay between silica fume, slag, and w/c ratio, providing valuable insights into their synergistic effects on concrete durability, particularly in resisting steel rebar corrosion. The ultimate goal is to formulate practical guidelines for the optimal utilization of these SCMs in producing robust and reliable concrete structures.

2 Materials and Methods

2.1 Preparation of Specimens

This study involved testing four distinct types of specimens to assess their performance. The first set of specimens involved incorporating silica fume as a partial replacement for cement, with w/cm ratios of 0.25, 0.3, 0.4, and 0.5. The purpose of these specimens was to investigate the influence of silica fume on steel corrosion in concrete exposed to chloride penetration. The second, third, and fourth sets of specimens comprised concrete mixes containing 20%, 30%, and 50% slag content as cement substitutes, with varying percentages of silica fume.

The w/cm ratios for these three sets of concrete specimens were 0.5, 0.4, and 0.3. The intention was to examine the effects of slag and the combined effects of slag and silica fume on steel corrosion in a chloride-rich concrete environment.

For each mix design, three specimens were designated for assessing steel corrosion by measuring half-cell potential. Furthermore, three specimens were devoted to determining the compressive strength at 28 days, and another three were used to determine the compressive strength at 91 days. Additionally, two specimens were employed to evaluate the depth of carbonation. Three additional 70-mm cubic specimens were prepared to fulfill specific testing requirements. Consequently, 728 specimens were manufactured, with 159 specimens designated for half-cell potential measurement, 15 for carbonation depth assessment, and the remaining specimens allocated to evaluate the compressive strength at 28 and 91 days.

2.2 Materials

The characteristics of cement, aggregate, and pozzolanic materials profoundly influence the mechanical properties and durability of High-Performance Concrete (HPC). Consistent with prior research, the following materials, selected based on specific criteria, were employed:

- Coarse broken limestone, adhering to the ASTM-C33 (Standard 2003) grading standard, with a maximum particle size of 12.5 mm, a dry density of 1950 kg/m^2, and a water absorption rate of 0.55%.
- Fine limestone, meeting the prescribed ASTM-C33 grading, with a density of 2.51 and a water absorption rate of 1%.
- The grain size distribution curves of the coarse and fine aggregates are shown in Fig. 1.
- Type 1 cement complied with the ASTM-C150 (Standard 2009) standard.
- Silica fume in powdered form, characterized by a density of 2.2.
- Slag of the type ground granulated blast furnace slag (GGBFS).
- Melamine–formaldehyde sulfate superplasticizer, following the specifications outlined in ASTM-C494 (Astm 2013).

2.3 Mix Design

2.3.1 Specimens with Silica Fume as a partial Cement Replacement

This set of specimens was explicitly designed to investigate the impact of silica fume on the corrosion of steel rebars exposed to chloride ions. Different proportions of silica fume (0%, 5%, 10%, and 15%) were partially replaced for

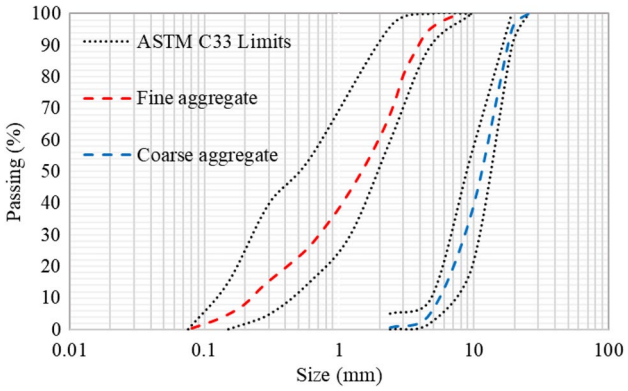

Fig. 1 Grain size distribution curves of coarse and fine aggregates

the cement content in each specimen at each w/cm ratio. The control specimen, in each w/cm ratio, contained 0% silica fume, serving as a reference against which the corrosion behavior of steel in other specimens was compared. A systematic coding system was employed to represent these specimens, using the letter 'A' to signify concrete with silica fume and no slag, followed by the respective w/cm ratio. Additionally, the proportion of silica fume incorporated in each specimen was indicated in the code. For instance, the code 'A 0.4–5' denoted a specimen with silica fume (without slag) at a w/cm ratio of 0.4, wherein 5% of the cement content was replaced by silica fume. Detailed mix designs for this group of specimens are presented in Table 1. Notably, the quantity of coarse aggregate in all specimens was kept constant at 1020 kg/m^2 to eliminate its influence on chloride ion penetration and subsequent steel corrosion.

2.3.2 Specimens with Slag and Silica Fume as Cement Replacements

This set of specimens was explicitly designed to investigate the effects of slag and a combination of slag and silica fume on steel corrosion in the presence of chloride ions. Cement was partially replaced with slag in these specimens at 20%, 35%, and 50%, respectively. Concurrently, silica fume was introduced as a substitute for cement at 0%, 5%, 10%, and 15% for each percentage of slag replacement.

To designate these specimens, the letters 'B', 'C' and 'D' were employed to represent concrete specimens containing 20%, 35%, and 50% slag content, respectively. The respective w/cm ratio was indicated, followed by the proportion of silica fume utilized. For example, the code 'D 0.3–10' referred to a specimen with 50% slag content and 10% silica fume, replacing a portion of the cement with a 0.3 w/cm ratio. In this instance, Portland cement constituted only 40% of the cementitious materials. The quantities of materials used in these specimens were consistent with those listed in Table 1, with the distinction being that groups B, C, and

Table 1 Concrete mix design variations (kg/m^3)

Specimen	*Added water	**SP%	Silica fume	Slag				Cement				Fine aggregates			
				A	B	C	D	A	B	C	D	A	B	C	D
(A, B, C, D) 0.5-0	202	1.1	0	0	76	133	190	380	304	247	190	692	685	680	675
(A, B, C, D) 0.5-5			19					361	285	228	171	685	679	674	669
(A, B, C, D) 0.5-10			38					342	266	209	152	679	672	667	662
(A, B, C, D) 0.5-15			57					323	247	190	133	672	665	660	656
(A, B, C, D) 0.4-0	184	1.5	0	0	86	151	215	430	344	279	215	695	687	681	676
(A, B, C, D) 0.4-5			21.5					408	322	258	193	687	680	674	668
(A, B, C, D) 0.4-10			43					387	301	236	172	680	672	667	661
(A, B, C, D) 0.4-15			64.5					365	279	215	150	672	665	659	654
(A, B, C, D) 0.3-0	174	1.8	0	0	108	189	270	540	432	351	270	629	620	613	606
(A, B, C, D) 0.3-5			27					513	405	324	243	620	611	604	597
(A, B, C, D) 0.3-10			54					486	378	297	216	611	601	594	587
(A, B, C, D) 0.3-15			81					459	351	270	189	602	592	585	578
A 0.25-0	162	2.8	0	0	–			600				605	–		
A 0.25-5			30					570				595			
A 0.25-10			60					540				585			
A 0.25-15			90					510				575			

*Water addition is based on a specific w/cm ratio and uses almost dry aggregate

**Percentage by weight of cementitious materials

The amount of coarse aggregate in all specimens is constant and equal to 1020 kg/m³

D incorporated 20%, 35%, and 50% slag replacement for cement, respectively.

2.4 Corrosion Tests of Steel in Concrete

2.4.1 Half-Cell Potential Measurement Device

This study evaluated steel bars' corrosion in concrete specimens through the half-cell potential measurement method, following the ASTM C876-91 standard (Astm 1999). As prescribed by this standard, if the potential measured using the copper/copper sulfate electrode exceeded 200 mV, there was a 90% probability that the steel rebars were free from corrosion. For potential values between 200 and 350 mV, the corrosion condition of the steel remained uncertain. Finally, if the measured potential fell below 350 mV, there was a 90% probability that corrosion had occurred in the steel rebars. The potential difference of the steel electrodes was compared to a copper–copper sulfate reference electrode, and the corrosion status of the steel was determined based on this potential difference.

When steel comes into contact with the pore solution inside the concrete, an electrochemical cell is formed, with the steel acting as the anode (where corrosion occurs) and the surrounding concrete acting as the cathode. In healthy concrete with a high pH (alkaline) environment, a thin, protective layer of iron oxide forms on the steel surface. This passive layer acts as a barrier, significantly hindering the corrosion process. The half-cell potential measurement assesses the electrical potential difference between the steel rebar and a reference electrode, reflecting the steel's tendency to corrode. A potential above 200 mV indicates a relatively high positive charge on the steel compared to the reference electrode, suggesting a stable passive layer effectively protecting the steel. A potential between 200 and 350 mV signifies an uncertain zone where the passive layer might be weakening or incipient corrosion might start. A potential below 350 mV suggests a relatively negative charge on the steel, indicating a breakdown of the passive layer, allowing the steel to readily participate in the corrosion process. At this stage, chloride ions and other aggressive elements in the pore solution can readily react with the steel, initiating the anodic dissolution of the steel.

The half-cell potential measurement device (see Fig. 2) comprises various components that must be assembled before utilization. These components include a voltmeter with high internal resistance, a reference electrode cylinder, a reference electrode, a surfactant tank, a base for supporting the voltmeter on the surfactant tank and connecting wires. Adhering to the manufacturer's instructions for the half-cell potential measurement device employed in this research, copper sulfate crystals were initially added to the antifreeze solution and thoroughly mixed. The resulting solution was then poured into the designated cylinder for the reference electrode. Ensuring that this solution always contains some insoluble copper sulfate is crucial. Subsequently,

Fig. 2 Half-cell potential measuring instruments

the reference electrode was positioned inside this cylinder and securely fastened with a screw at its end.

The surfactant tank was filled with contact electric solution, which was obtained by mixing 90 ml of contact electric material with 19 L of water. The solution needed to fill at least 75% of the tank's height. Following this, the cylinder containing the reference electrode was submerged in the solution within the surfactant tank, firmly closed, and secured with a screw at the end of the cylinder. The voltmeter base was then affixed to the end of the reference electrode cylinder outside the surfactant tank using a screw, and the voltmeter was placed atop it. The voltmeter was connected to the reference electrode through a connecting wire fixed to the base of the voltmeter. Additionally, the voltmeter base was connected to the reference electrode via the same screw beneath it. The reference electrode was connected to the voltmeter using a connecting wire to measure the half-cell potential. In contrast, another wire connected the steel rebar in the concrete specimen to the voltmeter. After a specified period, a steady numerical value was displayed on the digital voltmeter, indicating the potential of the rebar within the specimen relative to the reference electrode.

2.4.2 Environmental Conditions and Test Duration in Corrosion Testing

A seven-percent-by-weight NaCl solution created a chloride-rich environment conducive to corrosion. Distilled water prepared the NaCl solution, excluding extraneous substances that could influence steel corrosion. Additionally, a cyclic wetting and drying regime was implemented to expedite the corrosion of steel rebars embedded in the specimens. This regime involved subjecting the specimens to 48 h of exposure to ambient air once a week, facilitating water evaporation from their surfaces and pores. This process provided the necessary oxygen supply for steel corrosion.

Fig. 3 Carbonation depth measurement test device

The half-cell potential was measured for all fabricated specimens to compare the initiation times of corrosion among the specimens. The measurements were continued until their potentials dropped below 350 mV, indicating a 90% probability of steel corrosion. The test duration spanned approximately fifteen weeks, with weekly measurements conducted throughout this period. This comprehensive approach allowed for meticulously assessing the specimens' corrosion behavior and initiation times.

2.5 Measurement of Carbonation Depth

This research experimented to ascertain the carbonation depth in various specimens and investigate the influence of critical parameters, such as the w/cm ratio, silica fume percentage, slag percentage, and their combination, on carbonation depth. Since carbonation typically occurs at a slow rate under normal environmental conditions, an autoclave was employed to expedite the process (see Fig. 3). The concrete specimens were carefully placed in the autoclave tank. The lid was securely fastened using screws to ensure a complete seal. Subsequently, a CO_2 gas capsule was connected to the tank through a hose, and the specimens were subjected to a closed chamber saturated with CO_2 gas under a pressure of 1.5 atmospheres, the maximum reliable pressure for the autoclave device. This accelerated carbonation process lasted for one day. The pressure gauge on the chamber's lid indicated increased gas pressure. Once the pressure reached 1.5 atmospheres, the valve of the CO_2 gas capsule was closed. Over several days, the gas pressure gradually decreased, and it was periodically readjusted by opening and closing the valve of the capsule. After ten days, the specimens were removed from the autoclave and cut in half using a press.

A phenolphthalein reagent was applied to the fractured surfaces of the specimens to determine the depth of carbon dioxide penetration. The reagent, prepared by dissolving one gram of phenolphthalein powder in one liter of ethyl alcohol, facilitated the identification of regions of the concrete specimens that retained alkalinity (turning the colorless solution of phenolphthalein purple) and areas that had undergone carbonation (remaining unchanged in color). The carbonation depth was measured after one hour of applying the reagent to the fractured surfaces of the specimens, with gas penetration measured on all four sides of each specimen with a precision of 1 mm. The average penetration depth represented the carbonation depth for the respective mix design. Due to the limited volume of the autoclave device, two specimens were used for carbonation testing for each mix design, and the average penetration depth was considered the carbonation depth for that specific mix design.

2.6 Compressive Strength Analysis

The compressive strength analysis involved using seventy-mm-cubic specimens, as depicted in Fig. 4. These specimens were subjected to compressive strength testing at two distinct time intervals: 28 days and 91 days. Three specimens were prepared for each mixing design to ensure statistical validity and accuracy, resulting in 312 specimens specifically designated for compressive strength measurements. Moreover, additional specimens were made for each mixing design, replacing the original specimens if deemed unsuitable or compromised.

Fig. 4 Compressive strength test device

3 Results

3.1 Results of Half-Cell Potential Measurement

3.1.1 Specimens Without Slag

Figure 5a shows the results of monitoring the electrochemical potential of rebars in concrete specimens devoid of slag content (referred to as type A specimens). These specimens contain varying proportions of silica fume, with a constant w/cm ratio of 0.5. The figure depicts temporal variations in potential. The control specimen, which denotes the absence of silica fume, consistently exhibits lower potential values than specimens with silica fume, suggesting higher corrosion in the rebars of the control specimen.

The control concrete experienced a more rapid decline in potential below the 350 mV threshold, indicating a 90% probability of steel rebar corrosion according to ASTM C876 (Astm 1999). In contrast, the silica fume specimens showed a more extended delay before corrosion initiation, suggesting improved corrosion resistance. Consequently, the control concrete exhibits a shorter time to initiate corrosion, resulting in a higher corrosion rate. Notably, corrosion initiation in concrete containing 5% silica fume is superior to other silica fume proportions, thereby enhancing resistance to steel reinforcement corrosion.

Figure 5b illustrates the potential measurements within concrete specimens containing varying proportions of silica fume and a w/cm ratio of 0.4. Over three months, the internal rebar potential in the control specimen consistently remains lower than in specimens containing silica fume. This disparity highlights the superior corrosion resistance exhibited by silica fume-incorporated specimens. Notably, the control specimen experiences a more rapid decline below the 350 mV threshold than concrete containing 10% silica fume. Therefore, substituting 10% of cement with silica fume in the 0.4 w/cm ratio optimizes steel corrosion resistance. This enhanced resistance is likely attributed to the pozzolanic reaction of silica fume, which consumes calcium hydroxide, a byproduct of cement hydration, to form additional calcium silicate hydrate (C-S–H), the primary binding phase in concrete responsible for strength and durability.

Additionally, increasing silica fume content to 5% and 10% within w/cm ratios of 0.4 and 0.5 reduces the concrete's resistance to steel corrosion. This could be attributed to forming a denser microstructure at these ratios, which hinders the oxygen diffusion towards the steel rebar, which is essential for passivation. Conversely, raising silica fume content to 15% within the 0.15 w/cm ratio enhances the concrete's steel corrosion resistance. This

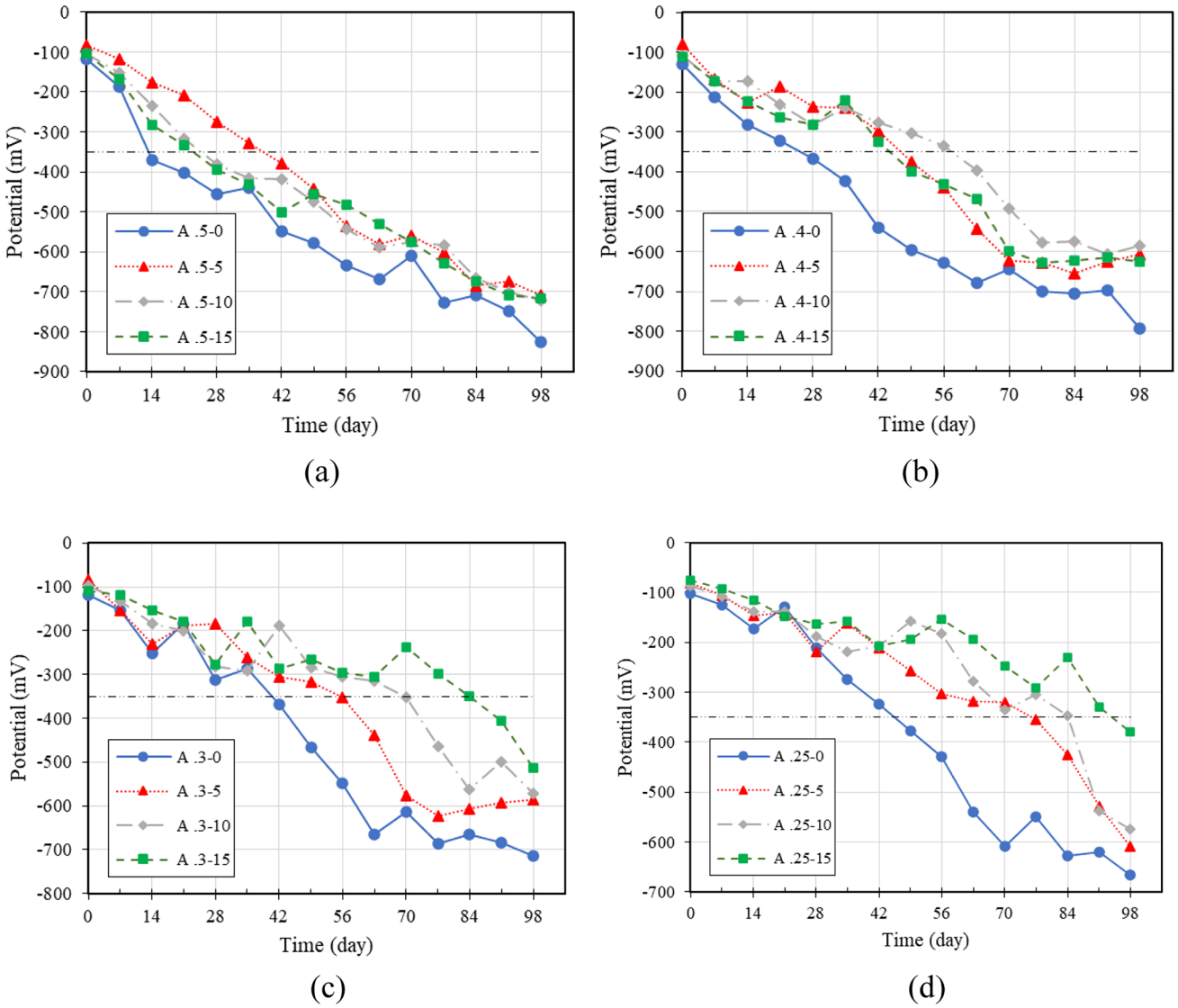

Fig. 5 Results of corrosion potential within type A specimens with different percentages of silica fume and w/cm ratios: **a** w/cm = 0.5; **b** w/cm = 0.4; **c** w/cm = 0.3; **d** w/cm = 0.25

is likely due to the reduced availability of free water for cement hydration at this lower ratio, leading to decreased calcium hydroxide production. The silica fume can effectively utilize this limited calcium hydroxide to form additional calcium silicate hydrate (C-S–H), improving the concrete's durability. Consequently, the optimal silica fume proportion for achieving peak concrete durability against steel corrosion varies dynamically in response to w/cm ratio adjustments. This dynamic relationship is crucial not only for enhancing corrosion resistance but also from an economic standpoint, considering the higher cost of silica fume compared to cement.

The following analysis, presented in Fig. 5c, focuses on type A concrete specimens with a w/cm ratio equal to 0.3. As silica fume proportions increase, the potential difference between control concrete and silica fume-containing specimens widens. This is accompanied by a more significant temporal separation in potential-time diagrams, indicating improved concrete performance against steel corrosion with increasing silica fume content. In this category, higher silica fume percentages simultaneously enhance the corrosion durability of the concrete. This could be attributed to the pozzolanic reaction of silica fume, which consumes calcium hydroxide, a byproduct of cement hydration, to form additional calcium silicate hydrate (C-S–H), the primary binding phase in concrete that imparts strength and durability. Notably, the time required for corrosion initiation in the 15% silica fume specimen exceeds that of other specimens, demonstrating superior corrosion resistance.

With a w/cm ratio of 0.25, as shown in Fig. 5d, increasing silica fume content improves concrete's performance and durability against steel corrosion. Specifically, the specimen with 15% silica fume consistently exhibits higher potential values across most measurement intervals, indicating superior corrosion resistance. Notably, reducing the w/cm ratio while increasing silica fume content further widens the gap in potential values between silica fume-infused concrete and the control, suggesting reduced susceptibility to corrosion in the former.

The reduction of the w/cm ratio significantly impacts rebar potential, hindering the migration of ions essential for corrosion initiation and thereby limiting corrosion susceptibility. This phenomenon arises from the denser and less permeable structure of the concrete. Notably, the extended time required for corrosion initiation enhances the longevity of the concrete structure. Additionally, increasing silica fume content and decreasing w/cm ratios further widen the potential gap between control and silica fume-incorporated concrete specimens, influencing corrosion resistance enhancement.

In conclusion, the interplay between a fixed proportion of silica fume and manipulated w/cm ratios dynamically influences rebar potential. This interaction plays a pivotal role in shaping concrete's corrosion susceptibility, with implications for its durability and structural longevity.

3.1.2 Specimens Containing 20% Slag

Figure 6a presents the results of measuring the potential of rebars within concrete specimens (type B) containing 20% slag as a partial cement substitute, various proportions of silica fume, and a fixed w/cm ratio of 0.5. Notably, the potential of rebars in concrete containing silica fume exhibited higher values compared to concrete with no silica fume, indicating reduced corrosion tendencies. This demonstrates that incorporating silica fume enhances concrete durability against steel corrosion in the presence of steel reinforcement. The specimen with 5% silica fume demonstrated superior performance, exhibiting a shorter time to corrosion initiation, albeit still longer than other silica fume-containing specimens. The specimens with 10% and 15% silica fume exhibited lower potential values than the 5% specimen but higher values than the 0% silica fume concrete. Furthermore, when comparing these specimens to similar ones (with 0.5 w/cm ratios and containing silica fume without slag), adding slag significantly improved the concrete's durability against steel corrosion. This suggests that utilizing both pozzolans, i.e., silica fume and slag, enhances concrete reliability against steel corrosion compared to using only silica fume.

Figure 6b presents the results of measuring the potential of rebars within type B concrete specimens with various proportions of silica fume and a fixed w/cm ratio of 0.4. The potential of rebars in specimens containing silica fume was consistently higher than in specimens with only slag and no silica fume, indicating improved corrosion resistance. The concrete specimen with 10% silica fume required more time for the rebars' potential to drop below 350 mV, indicating superior performance. This suggests that optimizing the silica fume percentage can improve concrete performance. This is likely due to the pozzolanic reaction of silica fume, which consumes calcium hydroxide (a by-product of cement hydration) to form an additional calcium silicate hydrate (C-S–H). C-S–H is the primary binding phase in concrete that provides strength and durability.

Reducing the w/cm ratio significantly impacts concrete's resistance to steel corrosion, as it reduces concrete's permeability. This, in turn, reduces the availability of water and oxygen for electrochemical reactions, thereby reducing steel corrosion rates. Consequently, concrete design guidelines should consider the required resistance factors and environmental conditions when selecting an appropriate w/cm ratio.

Figure 6c presents the results for type B concrete specimens with varying silica fume percentages and a 0.3 w/cm ratio. The corrosion potential of rebars embedded in concrete containing silica fume was consistently higher than rebars without silica fume. This difference in potential increased with higher silica fume percentages. The duration over which the potential remained above 200 mV served as an indicator of corrosion absence. In specimens with 10% and 15% silica fume, this period was approximately 1.5 and 2 times longer, respectively, compared to specimens without silica fume. Concrete with a 15% silica fume replacement exhibited superior performance, significantly delaying corrosion initiation. A plausible explanation for the observed outcomes is that adding silica fume reduces the concrete's permeability, impeding the penetration of chloride ions, the primary instigators of corrosion in reinforced concrete.

In practice, it is recommended to reduce the w/cm ratio to effectively utilize the properties of silica fume and slag to enhance concrete reliability against steel corrosion. Attention should be paid to proper compaction and curing during concrete construction, mainly when using silica fume, to prevent surface drying and cracking. In corrosive environments, cracks can facilitate the penetration of corrosive materials into the concrete. By carefully considering these factors, the durability and resistance of concrete against steel corrosion can be significantly improved.

3.1.3 Specimens Containing 35% Slag

Figure 7a illustrates the results of evaluating the corrosion potential of rebars embedded in type C concrete specimens

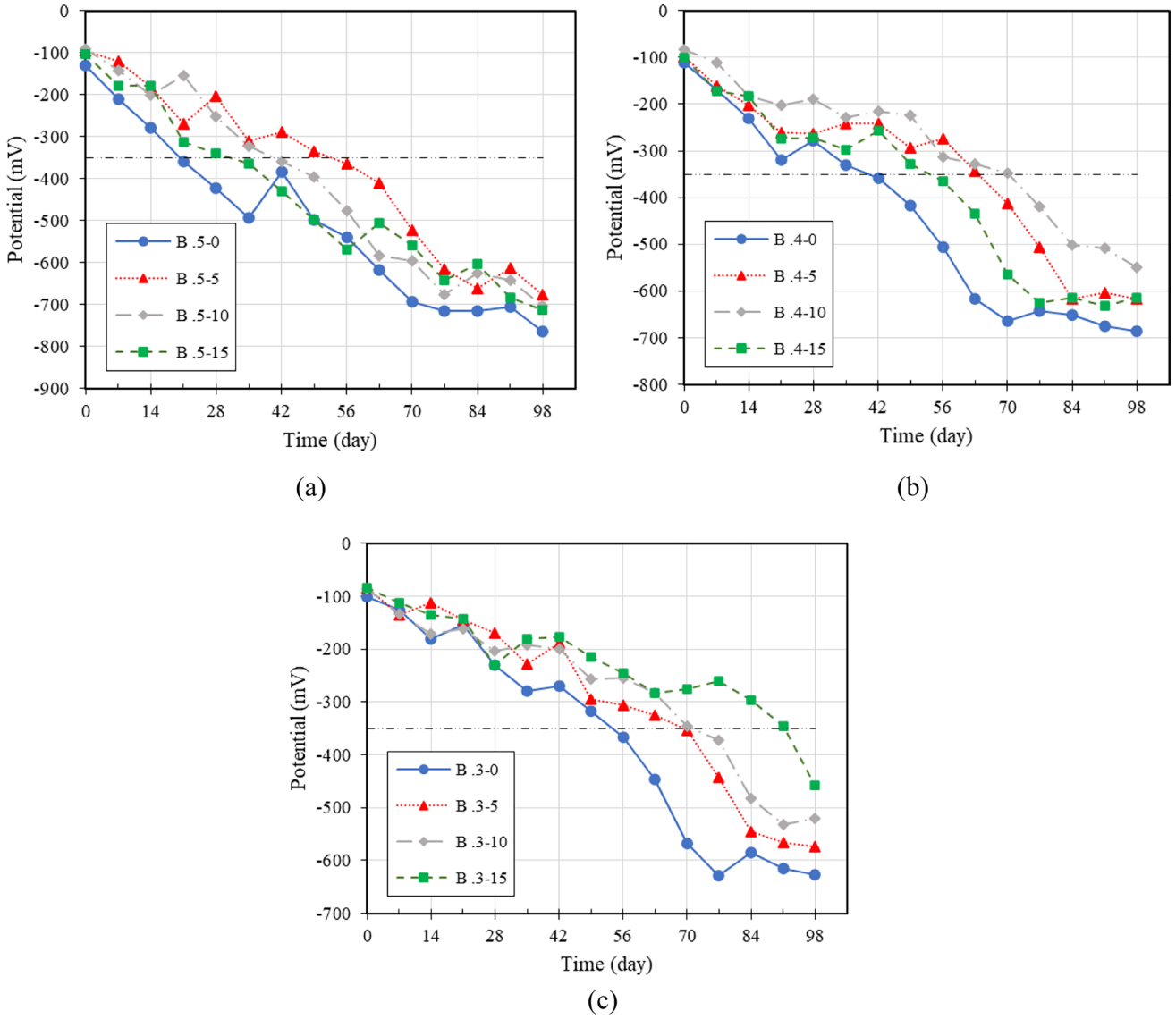

Fig. 6 Results of corrosion potential within type B specimens with different percentages of silica fume and w/cm ratios: **a** w/cm = 0.5; **b** w/cm = 0.4; **c** w/cm = 0.3

(with 35% slag as a partial cement replacement) containing varying amounts of silica fume while maintaining a constant w/cm ratio of 0.5. Notably, the concrete specimen containing 0% silica fume effectively represented a 35% slag replacement for cement.

The findings demonstrate that the specimen incorporating 5% silica fume exhibited a delayed onset of steel corrosion compared to other specimens, suggesting a lower corrosion rate. Specimens with 10% and 15% silica fume displayed similar corrosion onset times, outperforming those with 0%. Hence, adding silica fume, with 35% slag as a cement substitute, significantly enhances the concrete's resistance to steel corrosion. A comparison between type C specimens with a w/cm ratio of 0.5 and type A specimens containing no slag but with the same w/cm ratio highlights the superior performance of type C specimens. This advantage stems from the pozzolanic reaction of slag, which refines the concrete's microstructure, reduces permeability, and enhances its resistance against aggressive agents, including water and oxygen, essential for steel reinforcement corrosion. The pozzolanic reaction modifies the cement paste structure by converting calcium hydroxide crystals into hydrated calcium silicate (C-S–H), leading to denser concrete.

Additionally, Fig. 7b illustrates the results of measuring the rebar potential in type C concrete specimens with varying proportions of silica fume and a fixed w/cm ratio of 0.4. Here, the specimen containing 10% silica fume exhibited delayed corrosion onset compared to other specimens,

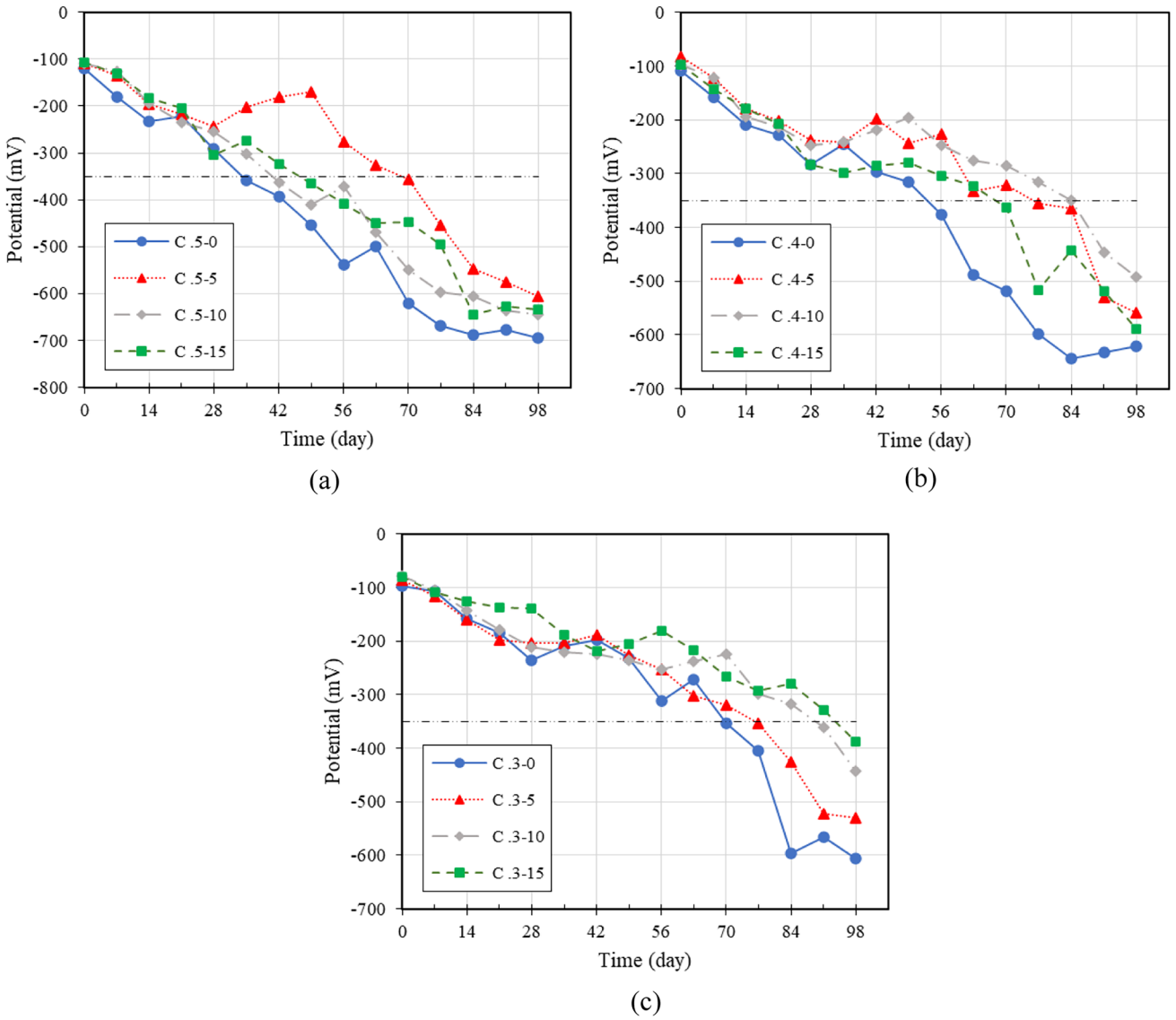

Fig. 7 Results of corrosion potential within type C specimens with different percentages of silica fume and w/cm ratios: **a** w/cm = 0.5; **b** w/cm = 0.4; **c** w/cm = 0.3

indicating enhanced durability against steel corrosion. Subsequently, the specimens with 5% and 15% silica fume performed better than those without silica fume. A comparison between the specimens containing 0% silica fume, which includes 35% slag as a cement substitute, and the specimen without slag and silica fume illustrates the beneficial impact of slag alone on the concrete's corrosion resistance. It is worth noting that although slag decreases the alkalinity of the concrete environment, which could increase the risk of corrosion, its ability to improve the concrete structure and reduce permeability outweighs this factor, ultimately increasing resistance to steel corrosion. Similarly, silica fume's pozzolanic properties contribute to converting calcium hydroxide into C-S–H, supporting the conclusion that adding silica fume to concrete specimens enhances their resistance against steel corrosion.

Furthermore, Fig. 7c displays the results of measuring the rebar potential in type C concrete specimens with varying amounts of silica fume and a fixed w/cm ratio of 0.3. Notably, the specimen containing 10% silica fume exhibited delayed onset of steel corrosion compared to other specimens, followed by the specimens containing 5% and 10% silica fume, respectively, showed better performance than those without silica fume. A closer examination of this figure reveals a reduced gap between the graph of the specimen without silica fume (with 35% slag substitution for cement) and those with silica fume, particularly in comparison to specimens containing 20% slag. This observation highlights

the superior corrosion performance of concrete with higher slag substitution (up to 35%). Additionally, when comparing these specimens with type B specimens, the increase in slag content from 20 to 35% substantially improved the concrete's resistance to steel corrosion. This economic significance lies in the fact that slag, a byproduct of the steel industry, incurs minimal cost, rendering it an affordable and cost-effective alternative to cement. Consequently, substituting cement with more significant slag in concrete construction saves costs. It confers beneficial effects such as enhanced corrosion and sulfate attack resistance, reduced hydration temperature, increased compressive strength, and decreased super-lubricant consumption.

3.1.4 Specimens Containing 50% Slag

In Fig. 8, the outcomes of assessing the rebar potential in type D concrete specimens (with varying percentages of slag as a cement substitute) with different proportions of silica fume and constant w/cm ratios of 0.5, 0.4 and 0.3, respectively, are presented. Figure 8a shows that the onset of corrosion in the concrete specimen containing 5% silica fume was delayed compared to other specimens. The corrosion onset time for concrete specimens containing 10% and 15% silica fume showed negligible differences, falling between the durations observed in the specimens with 5% and 0% silica fume.

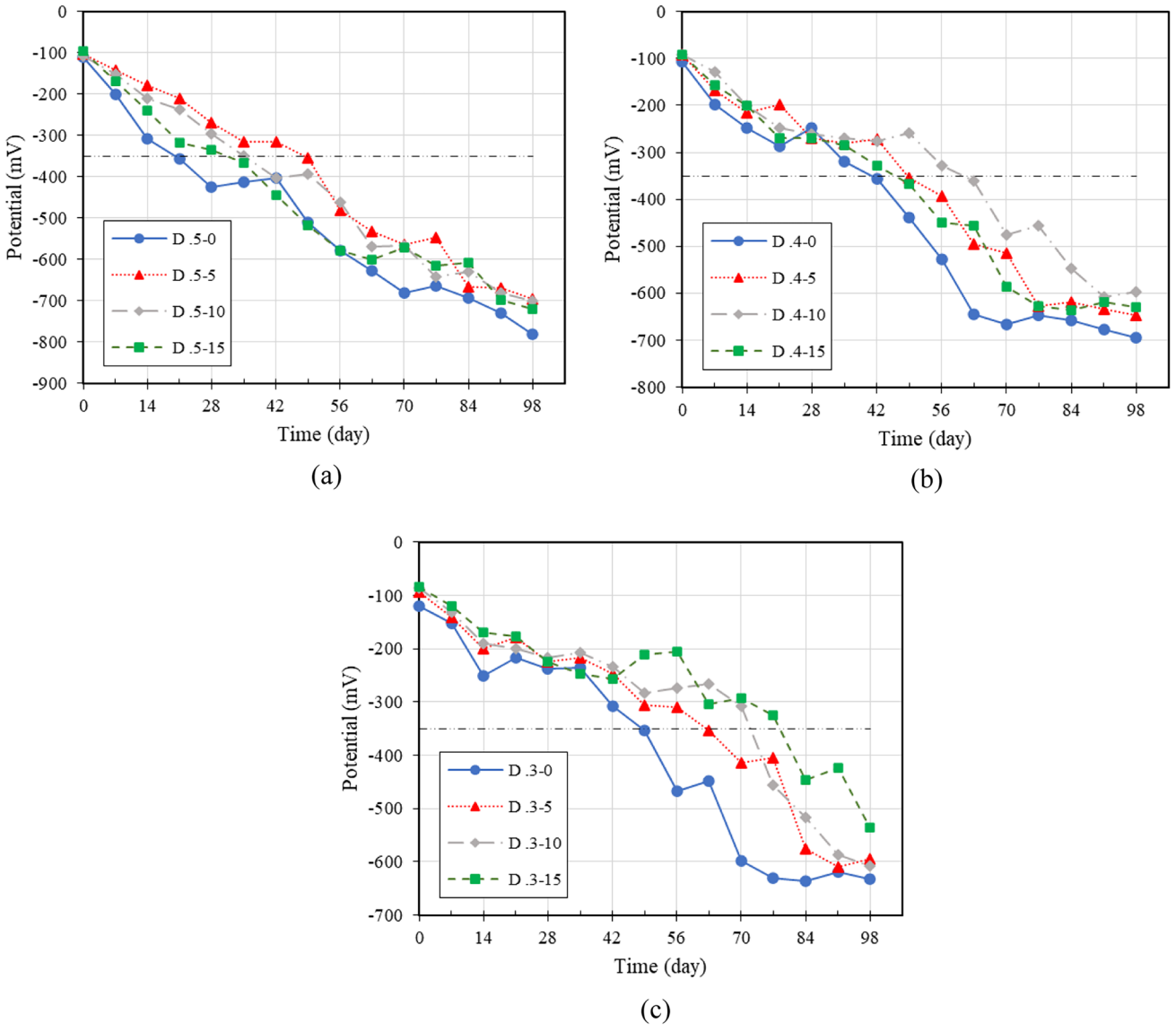

Fig. 8 Results of corrosion potential within type D specimens with different percentages of silica fume and w/cm ratios: **a** w/cm = 0.5; **b** w/cm = 0.4; **c** w/cm = 0.3

Figure 8b–c demonstrate that in type D specimens with w/cm ratios of 0.4 and 0.3, the incorporation of 10% and 15% silica fume yields the most favorable outcomes for enhancing concrete durability against steel corrosion. Across all type D specimens with different w/cm ratios, the combined use of silica fume and slag significantly improves concrete's resistance to steel corrosion compared to slag alone in concrete production.

It is worth noting that the potential difference between the specimens containing silica fume and slag decreased compared to cases where specimens solely contained silica fume, particularly evident at low w/cm ratios. This observation arises from the fact that slag in concrete enhances concrete's durability against steel corrosion. Although adding silica fume to the concrete mixture with slag increases its corrosion resistance, the effect of adding silica fume in this scenario is less pronounced than when added to concrete without slag. Nevertheless, the combined use of silica fume and slag consistently substantially improves concrete's resistance to steel corrosion than silica fume or slag in isolation.

The use of 50% slag as a cement substitute has adversely affected the durability of concrete against steel corrosion in most cases, as indicated by the shorter corrosion onset time compared to concrete with 20% slag. However, slag still protects concrete against steel corrosion relative to concrete without slag. This behavior is related to the impact of slag on the hydration and pore characteristics of the cement matrix, which determine the chloride transport and corrosion resistance of steel. Some studies have shown that slag can react with water and calcium hydroxide to produce more calcium silicate hydrate (C-S–H) and calcium aluminate hydrate (C-A-H), enhancing the concrete's density and strength. On the other hand, slag can also consume calcium hydroxide, which lowers the pore solution's pH value and reduces the concrete's alkalinity. This can impair the passivation ability of the concrete and increase the vulnerability of steel to corrosion. Furthermore, slag can raise the porosity and permeability of the concrete at early ages, allowing more chloride ions and oxygen to penetrate the concrete. These factors explain why concrete with 50% slag has poorer durability against steel corrosion than concrete with 20% slag or no slag. Nevertheless, concrete with 20% slag still outperforms concrete without slag because the positive effects of slag on the hydration products and the pore refinement dominate over the adverse impact of slag on the pH value and the porosity at later ages (Wang et al. 2020; Cao et al. 2019; Marcos-Meson et al. 2018; Otieno et al. 2016).

Previous research has indicated that the optimal content of silica fume ranges from 10 to 20% (Khan and Siddique 2011). In high-strength concretes, a 10% cement replacement with silica fume has been reported to yield the best results (Kayali and Zhu 2005). Various studies have shown that replacing cement with 20% to 50% slag can significantly enhance concrete's resistance to corrosion and chloride penetration (Song and Saraswathy 2006; Özbay et al. 2016). The results of the potential drop in this study indicate that the optimal content of slag in Group C, with 35% slag and 15% silica fume, resulted in a drop of 329 mV, which is below the threshold potential drop of 350 mV. Additionally, when comparing the two specimens, A-0.25–15 and C-0.3–15, which exhibited similar corrosion resistance at 91 days, it can be inferred that despite the lower water-to-cementitious materials (W/CM) ratio of specimen A-0.25–15 and the exact content of silica fume, replacing 35% of the slag not only maintains corrosion resistance but also offers environmental benefits in terms of reduced cement consumption.

3.1.5 Comparative Analysis of Time Required for Steel Corrosion Initiation

This study aimed to compare the time needed for steel corrosion to commence in different concrete specimens by establishing relationships between relevant variables. Consequently, a function was devised to express the initiation time of steel corrosion for two distinct concrete specimens based on the independent variables: w/cm ratio (W/CM), percentage of silica fume (SF/CM), and percentage of slag (Slag/CM) present in each of the compared specimens. Thus, this relationship involved six independent variables and one function (dependent variable), as Eq. (1) described.

$$\frac{(t_0)_1}{(t_0)_2} = F\left\{\left(\frac{W}{CM}\right)_1, \left(\frac{W}{CM}\right)_2, \left(\frac{SF}{CM}\right)_1, \left(\frac{SF}{CM}\right)_2, \left(\frac{Slag}{CM}\right)_1, \left(\frac{Slag}{CM}\right)_2\right\} \tag{1}$$

In Eq. (1), indices 1 and 2 pertain to the first and second specimens under comparison, respectively. The other parameters in this equation are W/CM, SF/CM, Slag/CM, and t0, which represent the time required for steel corrosion initiation.

Employing logarithmic interpolation, we derived Eq. (2) to facilitate comparing the time required for corrosion initiation between two distinct concrete specimens. This equation was formulated based on 1128 comparisons involving 1128 series of comparisons with the six independent variables and one dependent variable.

$$\frac{(t_0)_1}{(t_0)_2} = 1.346\left\{\frac{\left(\frac{W}{CM}\right)_2^{1.622}}{\left(\frac{W}{CM}\right)_1^{1.109}} \cdot \frac{\left(\frac{SF}{CM}\right)_1^{0.056}}{\left(\frac{SF}{CM}\right)_2^{0.078}} \cdot \frac{\left(\frac{Slag}{CM}\right)_1^{0.022}}{\left(\frac{Slag}{CM}\right)_2^{0.045}}\right\} \tag{2}$$

The above relationship allows for a preliminary estimation of the performance comparison of a concrete specimen against steel corrosion when compared to another concrete specimen while considering variations in the parameters of the w/cm ratio, percentage of slag, and percentage of silica fume as a replacement for cement.

If the effect of slag is disregarded in the observations, Eq. (3) is obtained. This relationship is based on 66 comparisons, which collectively encompass 66 series of comparisons.

$$\frac{(t_0)_1}{(t_0)_2} = 1.321\left\{\frac{\left(\left(\frac{W}{CM}\right)_2 + 1\right)^{4.36}}{\left(\left(\frac{W}{CM}\right)_1 + 1\right)^{3.403}} \cdot \frac{\left(\frac{SF}{CM}\right)_1^{0.05}}{\left(\frac{SF}{CM}\right)_2^{0.05}}\right\} \tag{3}$$

Equation (3) was derived from observations concerning concrete specimens containing only silica fume. Thus, when slag is not used in concrete production, and the parameters of w/cm ratio and the percentage of silica fume replacing cement are altered in two different specimens, Eq. (3) can be employed to compare the corrosion resistance performance of these two specimens.

Similarly, if the impact of silica fume is disregarded in the observations, Eq. (4) is derived. This relationship is also based on 66 comparisons.

$$\frac{(t_0)_1}{(t_0)_2} = 0.976\left\{\frac{\left(\left(\frac{W}{CM}\right)_2 + 1\right)^{5.099}}{\left(\left(\frac{W}{CM}\right)_1 + 1\right)^{3.166}} \cdot \frac{\left(\frac{Slag}{CM}\right)_1^{0.022}}{\left(\frac{Slag}{CM}\right)_2^{0.033}}\right\} - 1 \tag{4}$$

Equation (4) can be obtained by comparing the results of specimens containing only slag. Therefore, in cases where the w/cm ratio and the percentage of slag replacing cement vary, and no silica fume is present in the concrete, Eq. (4) can be used to estimate and compare the corrosion resistance performance of two different concretes.

The following restrictions for Eqs. (2), (3), and (4) are essential to note:

$$0 \le SF/CM \le 0.15,\ 0 \le Slag/CM \le 0.5,\ 0.3 \le W/CM \le 0.5. \tag{5}$$

During the internal stage of deriving Eqs. (2), (3), and (4), in cases where either SF/CM or Slag/CM became zero, logarithmic interpolation necessitated replacing zero with the value 0.0001. Hence, when using the equations mentioned earlier, if the percentage of slag or silica fume replacing cement in the specimens is zero, it is imperative to substitute zero with the value 0.0001 to ensure accurate calculations.

3.2 Carbonation Test

The carbonation test findings (Fig. 9) indicate that the incorporation of silica fume generally results in a negligible increase in carbonation depth compared to the control concrete in specimens containing 0% slag and varying w/c ratios. However, for w/c ratios of 0.3 and 0.25, the impact of silica fume addition on carbonation depth diminishes compared to ratios of 0.5 and 0.4, resulting in a minimal disparity between specimens with and without silica fume in terms of carbonation depth.

Conversely, when 20% of slag replaces cement, the carbonation depth decreases compared to similar specimens without slag. According to some research, slag can reduce the carbonation depth of concrete by enhancing the degree of hydration, refining the pore structure of the cement matrix, and raising the pore solution's pH value and buffering capacity (Zeyad et al. 2020; Tahwia et al. 2021). These effects, however, are more pronounced at lower slag contents (such as 20%) than at higher slag contents (such as 50%), as excess slag can increase the porosity and permeability of the concrete at early ages, facilitating carbon dioxide ingress and lowering the concrete's alkalinity.

On the other hand, silica fume can improve the carbonation resistance of concrete by decreasing the porosity and permeability of the cement matrix, as well as by forming additional calcium silicate hydrate (C-S–H) and calcium aluminate hydrate (C-A-H), which increase the density and strength of the concrete. However, these effects are more significant in concrete without slag than in concrete with slag because slag already provides some benefits to hydration products and pore structure refinement. Thus, adding silica fume has a negligible impact on the carbonation depth when 20% of slag substitutes for cement.

Conversely, when 50% of slag substitutes for cement, the carbonation depth increases compared to similar specimens without slag, and adding silica fume to the concrete composition slightly reduces the carbonation depth (Wei et al. 2023; Skibsted and Snellings 2019).

Increasing the slag content from 20 to 35% as a cement replacement leads to a reduction in carbonation depth compared to similar specimens containing 20% slag or no slag. Additionally, the inclusion of silica fume in the concrete mixture contributes to a decrease in carbonation depth, particularly compared to specimens containing 20% slag.

However, in concrete specimens with a slag content increased from 35 to 50%, the carbonation depth increases, in contrast to specimens containing 20% and 35% slag. Nevertheless, adding silica fume to concrete slightly decreases the carbonation depth in these specimens compared to concrete without silica fume.

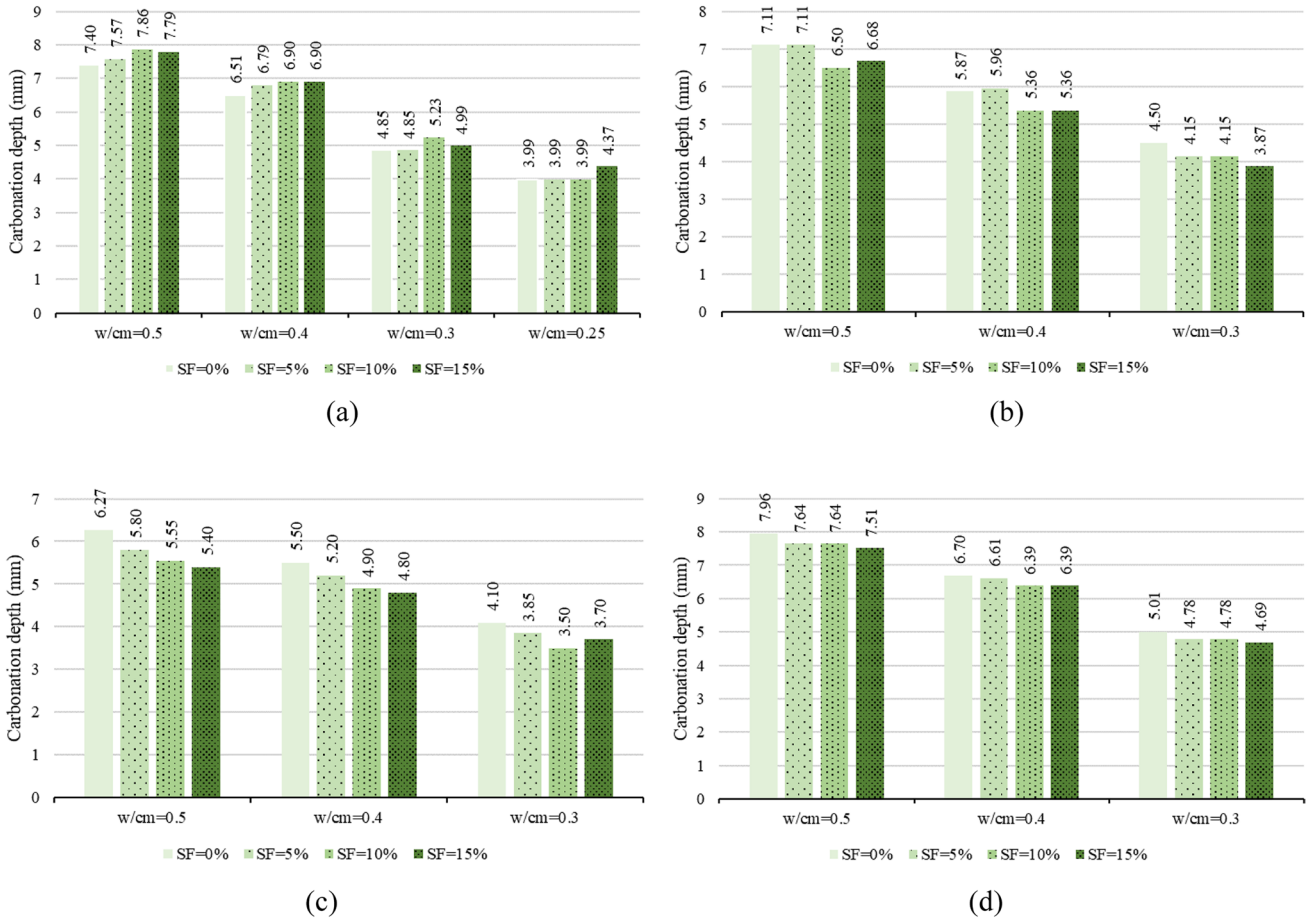

Fig. 9 Results of carbonation depth in different types of concrete specimens with varying percentages of silica fume and w/cm ratios: **a** Type A; **b** Type B; **c** Type C; **d** Type D

3.3 Compressive Strength

Figure 10 displays the compressive strength of type A concrete specimens containing various proportions of silica fume while maintaining constant w/cm ratios of 0.5, 0.4, 0.3, and 0.25. By comparing the compressive strength of 91-day specimens with that of 28-day specimens, it becomes apparent that the majority of concrete's compressive strength is achieved by 28 days, with specimens containing silica fume consistently exhibiting higher compressive strengths than control specimens. Among the specimens with a w/cm ratio of 0.5, the specimen containing 10% silica fume demonstrated the highest compressive strength at 28 and 91 days. In the case of a w/cm ratio of 0.25, while the 28-day compressive strength of the specimen with 10% silica fume was slightly superior to that with 15% silica fume, the 91-day compressive strength of the specimen containing 15% silica fume surpassed that of the 10% silica fume specimen. Therefore, for w/cm ratios, incorporating 15% silica fume in the concrete mixture leads to the highest compressive strength at 91 days, followed by specimens with 10% and 5% silica fume.

Moreover, the research results indicate that when using limestone aggregates with w/cm ratios of 0.3 and 0.4, substituting 10% silica fume in cement yields the most significant increase in concrete's compressive strength. However, for concrete with a w/cm ratio of 0.25, replacing cement with 15% silica fume exhibits higher compressive strength than 10%. One possible reason for the results shown in Fig. 10 is that silica fume has a pozzolanic effect on the hydration of cement, which means that it reacts with the calcium hydroxide released by the cement hydration and forms additional calcium silicate hydrate (C-S–H), the primary binding phase in concrete. This improves the cement paste's density, strength, and durability, enhancing the compressive strength of concrete.

The optimal dosage of silica fume depends on the w/cm ratios and the curing time of the concrete. Silica fume can increase the water demand and reduce the workability of fresh concrete, especially at higher dosages and lower w/cm ratios. This can affect the quality of compaction and

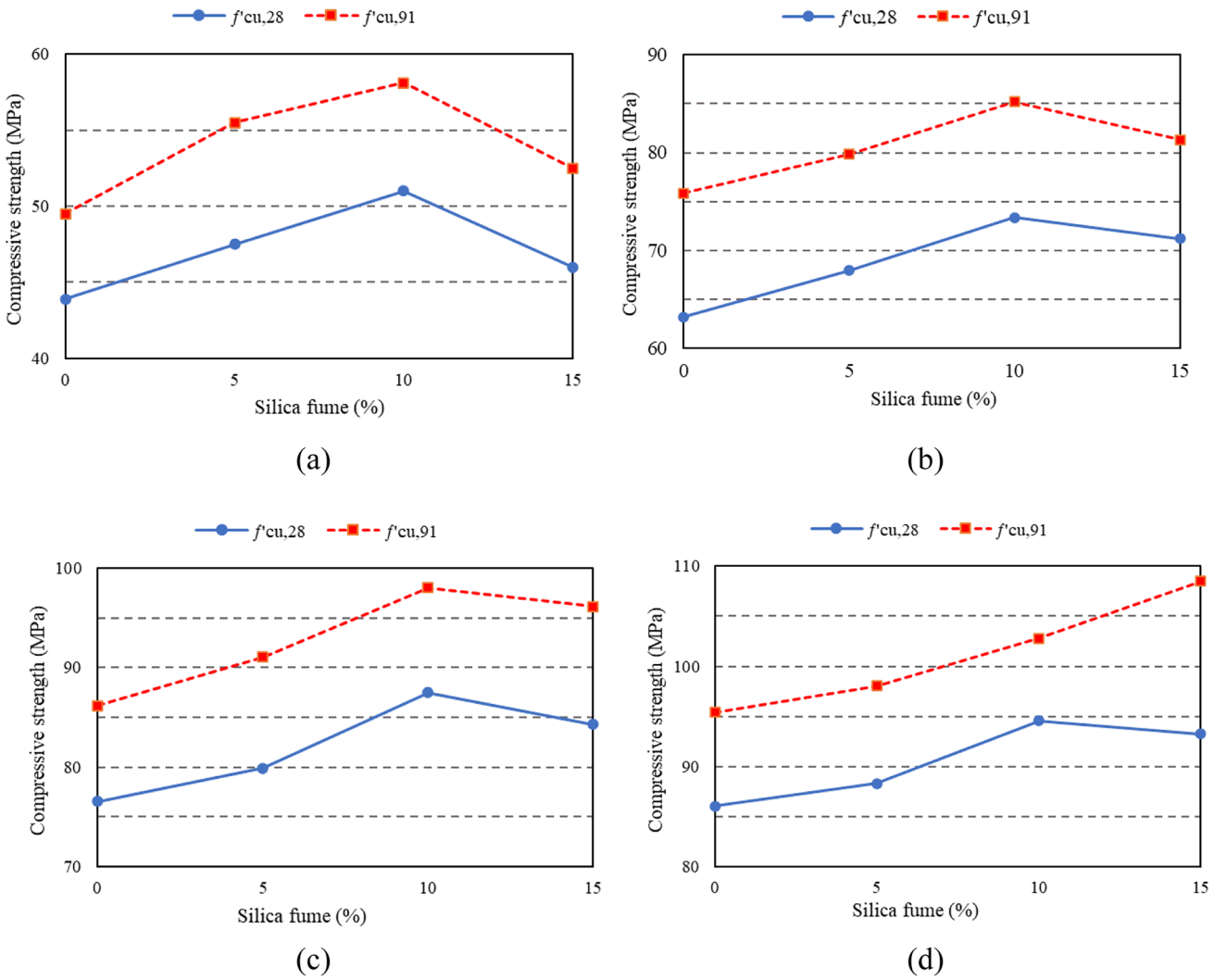

Fig. 10 Compressive strength of type A specimens with different percentages of silica fume and w/cm ratios: **a** w/cm = 0.5; **b** w/cm = 0.4; **c** w/cm = 0.3; **d** w/cm = 0.25

consolidation, potentially reducing compressive strength. Therefore, for higher w/cm ratios, such as 0.5, a lower dosage of silica fume, like 10%, may suffice to achieve maximum compressive strength. Conversely, for lower w/cm ratios, such as 0.25, a higher dosage of silica fume, like 15%, may be necessary to counteract the adverse effects of low water content and high cement content on concrete's hydration process and pore structure.

Silica fume can accelerate early strength development in concrete. Still, its long-term strength gain may be slower than plain concrete due to the reduced availability of calcium hydroxide for further pozzolanic reaction. For longer curing times, such as 91 days, a higher dosage of silica fume, like 15%, may be more beneficial than a lower dosage, like 10%, to achieve higher compressive strength, especially for lower w/cm ratios, such as 0.25. These factors may explain why, for w/cm ratios of 0.3 and 0.4, incorporating 10% silica fume in the concrete mixture leads to the highest compressive strength at both 28 and 91 days, while for a w/cm ratio of 0.25, replacing cement with 15% silica fume exhibits higher compressive strength at 91 days compared to 10% (Uddin et al. 2023; Albattat et al. 2020).

A comparison of the optimum silica fume percentages in type A specimens with varying w/cm ratios indicates that reducing the w/cm ratio improves the performance of specimens with higher silica fume contents in terms of compressive strength. In Fig. 11, the compressive strength results of type B concrete specimens containing different percentages of silica fume are presented, with fixed w/cm ratios of 0.5, 0.4, and 0.3. The outcomes reveal that including silica fume in concrete containing slag enhances the compressive strength of specimens. The order of increasing compressive strength in specimens with silica fume remains consistent

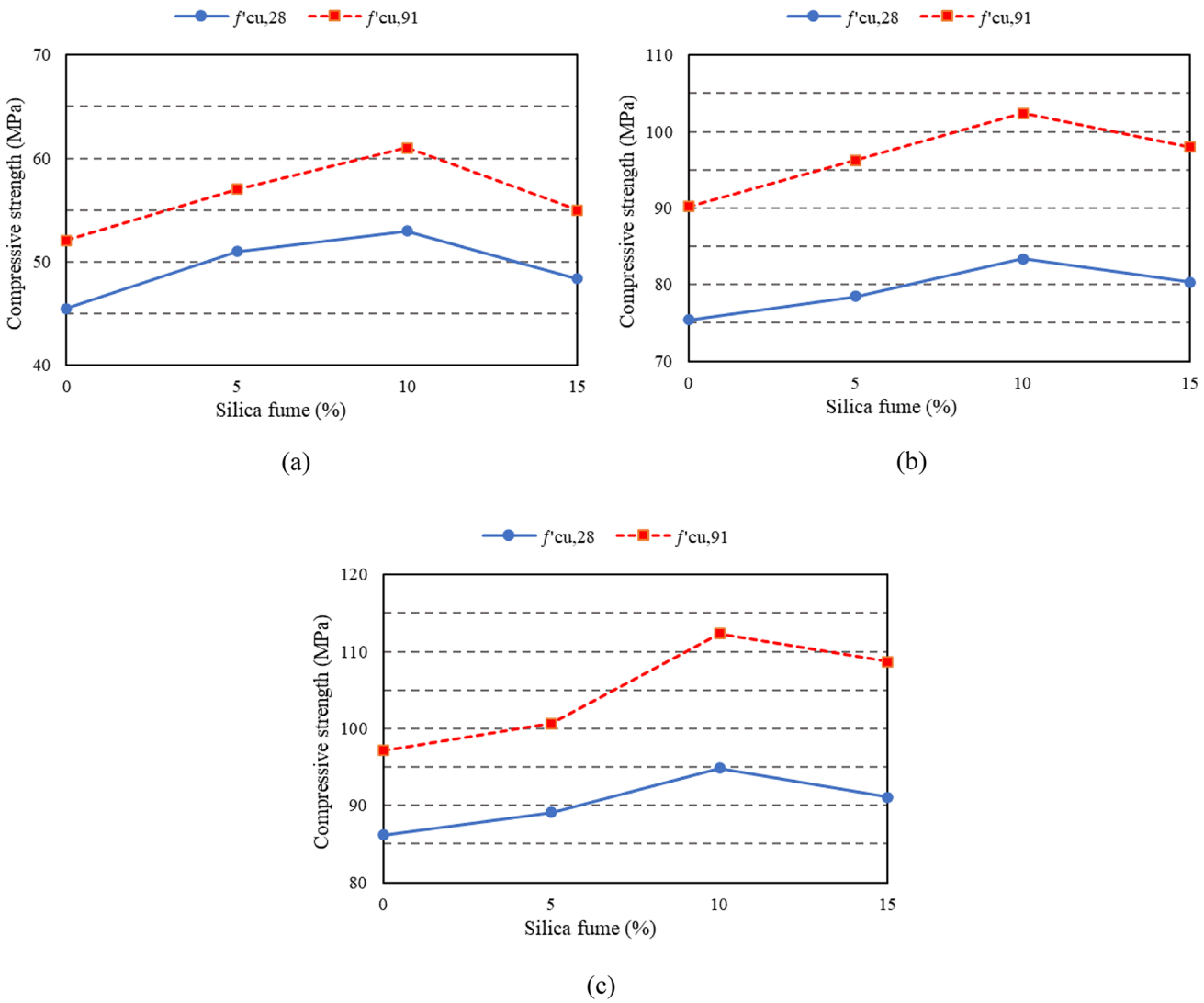

Fig. 11 Compressive strength of type B specimens with different percentages of silica fume and w/cm ratios: **a** w/cm = 0.5; **b** w/cm = 0.4; **c** w/cm = 0.3

across each w/cm ratio, mirroring the trend observed in type A specimens.

Figure 12 demonstrates the compressive strength results of concrete specimens with varying silica fume percentages and w/cm ratios of 0.5, 0.4, and 0.3, respectively. Notably, the 28-day compressive strength of type C specimens was lower than similar specimens with 20% slag (type B) and even specimens without slag (type A). This discrepancy can be attributed to the slower hydration reaction of slag, resulting in reduced strength development in cement with slag compared to regular cement without slag. However, once the slag hydration reaction is completed, the microstructure of the concrete improves, leading to higher strength in concrete containing slag compared to concrete without slag. As seen in the results, the 91-day compressive strength of concrete containing slag (especially in the case of type C specimens) becomes comparable to specimens without slag and even specimens with 20% slag. Thus, it can be inferred that the slag hydration reaction occurred before 28 days in type B specimens, resulting in higher 28-day compressive strength than in specimens without slag. However, in type C specimens, where the percentage of slag replacement increased, more time was required for the slag hydration reaction to complete in the concrete mixture. It is worth mentioning that the slow rate of slag hydration reaction contributes to reduced heat development in concrete, which may be advantageous during mass concreting. In type C specimens, the optimum percentages of silica fume in each w/cm ratio align with type B specimens, with the strength of specimens containing silica fume exhibiting improvement compared to those without it.

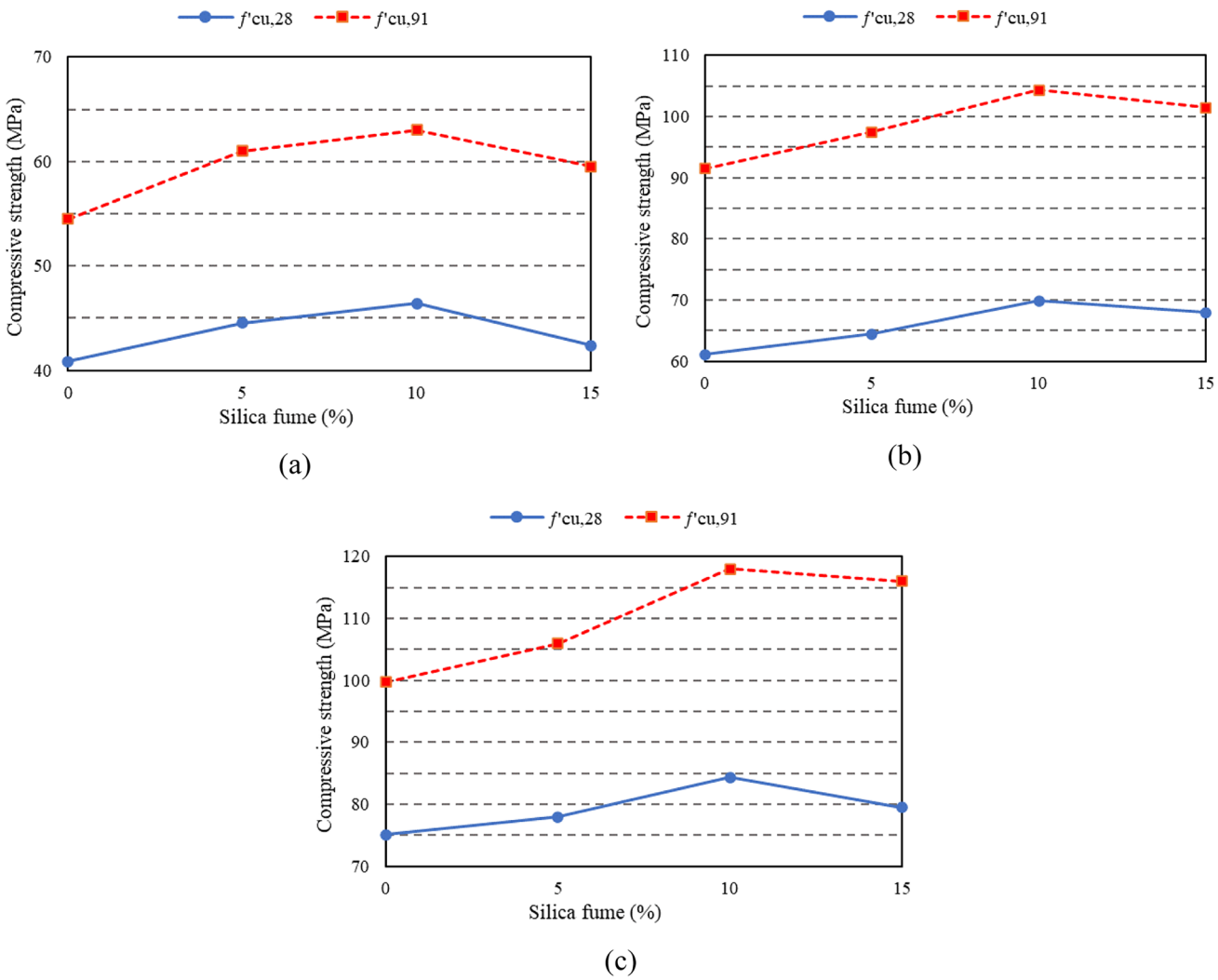

Fig. 12 Compressive strength of type C specimens with different percentages of silica fume and w/cm ratios: **a** w/cm = 0.5; **b** w/cm = 0.4; **c** w/cm = 0.3

The results suggest that the slag content in concrete influences the hydration process and the pore structure of the cement matrix, which affects the compressive strength of concrete. Some studies have shown that slag can react with water and calcium hydroxide to produce more calcium silicate hydrate (C-S-H) and calcium aluminate hydrate (C-A-H), enhancing the density and strength of the concrete. However, slag can also consume calcium hydroxide, lowering the pore solution's pH value and reducing the concrete's alkalinity. This can impair the passivation ability of the concrete and increase the vulnerability of steel to corrosion. Furthermore, slag can increase the porosity and permeability of the concrete at early ages, allowing more chloride ions and oxygen to penetrate the concrete. These factors account for why concrete with slag (especially in the case of type C specimens) has poorer compressive strength than concrete without slag at 28 days. However, as the curing time progresses, the slag hydration reaction fills the pores in the cement matrix, improving the compressive strength of concrete. Therefore, at 91 days, concrete with slag becomes similar to or even higher than concrete without slag in terms of compressive strength. Adding silica fume to the concrete mixture can further improve the compressive strength by decreasing the porosity and permeability of the cement matrix, as well as by forming additional C-S-H and C-A-H. The optimal dosages of silica fume depend on the w/cm ratios and the slag content in the concrete mixture (Chen and Brouwers 2007; Powers and Brownyard 1946).

Figure 13 illustrates the compressive strength results of type D concrete specimens containing different percentages of silica fume, with w/cm ratios of 0.5, 0.4, and 0.3, respectively. In this specimen type, 50% of cement was substituted with slag, and with the addition of silica fume to the concrete, the strength of type D specimens, similar to type A, B, and C specimens,

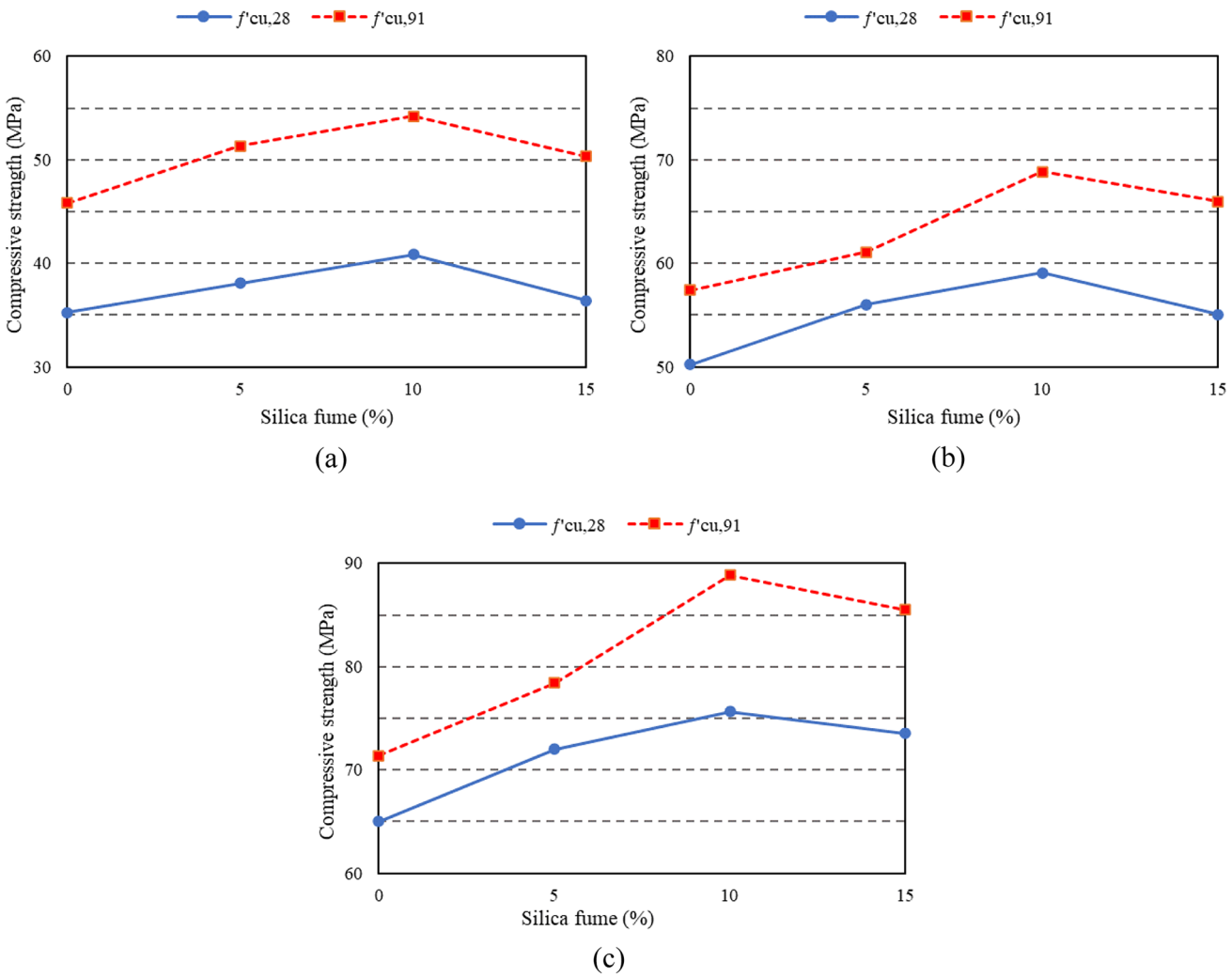

Fig. 13 Compressive strength of type D specimens with different percentages of silica fume and w/cm ratios: **a** w/cm = 0.5; **b** w/cm = 0.4; **c** w/cm = 0.3

increased compared to concrete without silica fume. Notably, the compressive strength and the rate of strength gain in concrete containing slag may vary significantly. By comparing the slag-containing samples, it can be concluded that the optimal slag content, according to the results of this study, is 35%. Additionally, the synergistic effect of 35% slag combined with 10% silica fume at a w/cm ratio of 0.3 results in the highest increase in compressive strength. Overall, using 35% slag and 10–15% silica fume exhibits the most significant synergistic effect across all w/cm ratios.

Previous studies show that 20% slag replacement often yields the best results in increasing the compressive strength. The compressive strength of the concrete increased by 5% and 21% at 28 and 90 days, respectively, compared to the reference concrete at 28 days without GGBS (Ahmad et al. 2022; Ganesh and Murthy 2019). Substituting 10% silica fume increased the strength by 21% and 17% at 28 and 90 days, respectively (Mazloom et al. 2004; Wong and Razak 2005). This study identifies the optimal combination for compressive strength, where a specimen containing 35% slag and 10% silica fume with a w/cm of 0.3 showed a 37% increase in strength compared to the control specimen (A-0.3-0). This comparison confirms that SF and GGBFS, through improved microstructural and grain-size distribution, aid in better-adjusting pressure distribution mechanisms and load distribution within the concrete matrix. Additionally, the differing rates of short-term and long-term pozzolanic reactions in silica fume and slag-containing concrete contribute to their synergy in the long term, resulting in a more pronounced increase in concrete compressive strength compared to when used separately.

4 Conclusions

This study investigated the influence of silica fume and slag and their interaction effects on steel corrosion, carbonation depth, and compressive strength of concrete. Four groups of concrete specimens were designed and cast. The first group contained only silica fume with different water-to-cement (w/cm) ratios (0.25, 0.3, 0.4, and 0.5). Groups two, three, and four incorporated 20%, 35%, and 50% slag as a cement replacement, respectively, along with varying percentages of silica fume and w/cm ratios of 0.3, 0.4, and 0.5. The key findings of the research are summarized as follows:

1. Using silica fume in concrete enhances compressive strength by promoting pozzolanic reactions that produce more calcium silicate hydrate and reduce calcium hydroxide. Additionally, silica fume fills pores and improves the microstructure of the concrete, thereby reducing permeability and increasing durability against corrosive elements. Among specimens in the first category, A-0.25-15, with a w/cm ratio of 0.25 and 15% cement replaced by silica fume, exhibited the highest corrosion resistance (91 days). This specimen did not exceed the threshold level of -350 mV and showed a nearly 46.7% increase in corrosion resistance compared to a similar specimen without silica fume (A-0.25-0).
2. Among specimens containing slag, specimen C-0.3-15 exhibited the highest corrosion resistance, with a corrosion potential of -329 mV after 91 days. This specimen demonstrated a 19% and 44% increase in corrosion resistance compared to similar specimens without slag (A-0.3-15) and silica fume (C-0.3-0), respectively.
3. The results revealed that increasing slag content by up to 35% reduced carbonation depth. Conversely, incorporating 50% slag resulted in a significant increase in carbonation depth compared to specimens containing lower slag contents, performing nearly similar to Group A (without slag) specimens. Furthermore, the results indicated that including silica fume within 10–15% across all groups, with or without slag, decreased the carbonation depth.
4. Specimen C-0.3-10 exhibited the lowest carbonation depth, recording a value of 3.5 mm. Notably, this specimen demonstrated a 33% and 14.6% reduction in carbonation depth compared to specimens A-0.3-10 (similar concrete without slag) and C-0.3-0 (similar specimen without silica fume), respectively.
5. Specimen C-0.3-10 exhibited the highest compressive strength, equal to 118 MPa. This value represented a 20.4% increase compared to the counterpart concrete specimen without slag (A-0.3-10) and an 18.4% enhancement in strength relative to the similar specimen lacking silica fume (C-0.3-0).
6. Using 50% slag as a cement substitute negatively impacts concrete durability, especially against steel corrosion, due to shorter corrosion onset times. This high slag content lowers pH and alkalinity, increasing porosity and permeability and allowing more chloride ions and oxygen to penetrate. This leads to poorer corrosion resistance and compressive strength than concrete with lower slag. However, it has almost the same performance as a specimen without slag.
7. Combining silica fume and slag as partial cement replacements enhanced concrete performance by refining pore structure, reducing permeability, and increasing pozzolanic reactions. This study found the optimal combination in Group C with 35% slag and 10-15% silica fume. Utilizing this optimal mixed design of slag and silica fume and their synergistic effect improved durability and compressive strength, reduced cement consumption, and provided environmental benefits.

Author contributions Conceptualization and design of the study: (Davood Mostofinejad), (Mohsen Nasrollahi) Data collection: (Morteza Sadeghi), (Zahra Zajshoor) Analysis and interpretation of results: (Mohsen Nasrollahi), (Hadi Bahmani), Drafting the initial manuscript: (Mohsen Nasrollahi) Review and final editing: (Davood Mostofinejad), (Mohsen Nasrollahi) Supervisor:(Davood Mostofinejad).

Funding Isfahan University of Technology.

Data availability No datasets were generated or analysed during the current study.

Declarations

Conflict of interest The authors declare no competing interests.

References

ACI Committee, C. of M. in Concrete, (1975) Corrosion of metals in concrete, In: American Concrete Institute

Ahmad J, Kontoleon KJ, Majdi A, Naqash MT, Deifalla AF, Ben Kahla N, Isleem HF, Qaidi SMA (2022) A comprehensive review on the ground granulated blast furnace slag (GGBS) in concrete production. Sustainability. 14:8783

Aitcin P-C (1993) High-performance concrete demystified. Concr Int 15:21–26

Albattat RAI, Jamshidzadeh Z, Alasadi AKR (2020) Assessment of compressive strength and durability of silica fume-based concrete in acidic environment. Innov Infrastruct Solut 5:1–7

Al-Saadoun SS, Al-Gahtani AS (1992) Reinforcement corrosion-resisting characteristics of silica-fume blended-cement concrete. Mater J 89:337–344

ASTM C (1999) Standard test method for half-cell potentials of uncoated reinforcing steel in concrete. ASTM C 876–91

ASTM C (2013) Standard specification for chemical admixtures for concrete. Annu. B. ASTM Stand

Bahmani H, Mostofinejad D (2023) A review of engineering properties of ultra-high-performance geopolymer concrete. Dev. Built Environ 14:100126

Bahmani H, Mostofinejad D (2022) Microstructure of ultra-high-performance concrete (UHPC)–a review study. J Build Eng 50:104118
Bayasi Z, Zhou J (1993) Properties of silica fume concrete and mortar. Mater J 90:349–356
Berke NS (1989) Resistance of microsilica concrete to steel corrosion erosion and chemical attack. Spec Publ 114:861–886
Cao Y, Gehlen C, Angst U, Wang L, Wang Z, Yao Y (2019) Critical chloride content in reinforced concrete—an updated review onsidering Chinese experience. Cem Concr Res 117:58–68
Chen W, Brouwers HJH (2007) The hydration of slag, part 2: reaction models for blended cement. J Mater Sci 42:444–464
Chuang ML, Huang WH (2013) Durability analysis testing on reactive powder concrete. Adv Mater Res 811:244–248
Ganesh P, Murthy AR (2019) Tensile behaviour and durability aspects of sustainable ultra-high performance concrete incorporated with GGBS as cementitious material. Constr Build Mater 197:667–680
Ghanbari MA, Amirabdollahian A, Asayesh S, Nasri M, Mehri B, Shirzadi Javid AA (2023) Durability evaluation of binary and ternary concrete mixtures by corrosion resistance approach. Adv. Struct. Eng. 26:1325–1337
Hajiaghamemar M, Mostofinejad D, Bahmani H (2022) High volume of slag and polypropylene fibres in engineered cementitious composites: microstructure and mechanical properties. Mag Concr Res 75:607–624
Hooton RD (1993) Influence of silica fume replacement of cement on physical properties and resistance to sulfate attack, freezing and thawing, and alkali-silica reactivity. Mater J 90:143–151
Huang R, Yang CC (1997) Condition assessment of reinforced concrete beams relative to reinforcement corrosion. Cem Concr Compos 19:131–137
Iravani S (1996) Mechanical properties of high-performance concrete. Mater J 93:416–426
Kayali O, Zhu B (2005) Corrosion performance of medium-strength and silica fume high-strength reinforced concrete in a chloride solution. Cem Concr Compos 27:117–124
Khan MI, Siddique R (2011) Utilization of silica fume in concrete: review of durability properties. Resour Conserv Recycl 57:30–35
Kurtis KE, Mehta K (1997) A critical review of deterioration of concrete due to corrosion of reinforcing steel. Spec Publ 170:535–554
Li S, Roy DM (1986) Investigation of relations between porosity, pore structure, and C1−diffusion of fly ash and blended cement pastes. Cem Concr Res 16:749–759
Li Z, Peng J, Ma B (1999) Investigation of chloride diffusion for high-performance concrete containing fly ash, microsilica, and chemical admixtures. Mater J 96:391–396
Marcos-Meson V, Michel A, Solgaard A, Fischer G, Edvardsen C, Skovhus TL (2018) Corrosion resistance of steel fibre-reinforced concrete-a literature review. Cem Concr Res 103:1–20
Mazloom M, Ramezanianpour AA, Brooks JJ (2004) Effect of silica fume on mechanical properties of high-strength concrete. Cem Concr Compos 26:347–357
Mehri B, Shirzadi Javid AA, Asayesh S, Ghanbari MA (2023) The assessment of durability, coefficient of thermal expansion, and bonding strength of latex modified mixtures in repairing restrained concrete pavements. Int. J. Pavement Eng. 24:2048301
Mohd Faizal MJ, Hamidah, MS, Muhd Norhasri MS, Noorli I (2016) Effect of clay as a nanomaterial on corrosion potential of steel reinforcement embedded in ultra-high performance concrete, In: InCIEC 2015 Proc. Int. Civ. Infrastruct. Eng. Conf., Springer, pp. 679–687.
Osborne GJ (1992) Durability of blast furnace slag cement concretes, Build Res Establishment
Otieno M, Beushausen H, Alexander M (2016) Chloride-induced corrosion of steel in cracked concrete–Part I: experimental studies under accelerated and natural marine environments. Cem Concr Res 79:373–385
Özbay E, Erdemir M, Durmuş Hİ (2016) Utilization and efficiency of ground granulated blast furnace slag on concrete properties–a review. Constr Build Mater 105:423–434
Ozyildirim C (1993) High-performance concrete for transportation structures. Concr Int 15:33–38
Pettersson K, Sandberg P (1997) Chloride threshold levels, corrosion rates and service life for cracked high-performance concrete. Spec Publ 170:451–472
Pigeon M, Garnier F, Pleau R, Aitcin P-C (1993) Influence of drying on the chloride ion permeability of HPC. Concr Int 15:65–69
Powers TC, Brownyard TL (1946) Studies of the physical properties of hardened Portland cement paste, In: J. Proc. pp. 101–132.
Scanton JM, Sherman MR (1996) Fly ash concrete: An evaluation of chloride penetration testing methods. Concr Int 18:57–62
Skibsted J, Snellings R (2019) Reactivity of supplementary cementitious materials (SCMs) in cement blends. Cem Concr Res 124:105799
Song H-W, Saraswathy V (2006) Studies on the corrosion resistance of reinforced steel in concrete with ground granulated blast-furnace slag—an overview. J Hazard Mater 138:226–233
Standard A (2003) Standard specification for concrete aggregates. ASTM Int 1:11
Standard A (2009) Standard specification for Portland cement, ASTM Int. West Conshohocken, PA
Tahwia AM, Elgendy GM, Amin M (2021) Durability and microstructure of eco-efficient ultra-high-performance concrete. Constr Build Mater 303:124491
Torll K, Sasatani T, Kawamura M (1995) Effects of fly ash, blast furnace slag, and silica fume on resistance of mortar to calcium chloride attack. Spec Publ 153:931–950
Uddin MA, Bashir MT, Khan AM, Alsharari F, Farid F, Alrowais R (2023) Effect of silica fume on compressive strength and water absorption of the Portland cement-silica fume blended mortar. Arab. J. Sci. Eng. 49:1–9
Voo YL, Foster SJ (2010) Characteristics of ultra-high performance 'ductile' concrete and its impact on sustainable construction, IES. J Part A Civ Struct Eng 3:168–187
Wang J, Xie J, Wang C, Zhao J, Liu F, Fang C (2020) Study on the optimum initial curing condition for fly ash and GGBS based geopolymer recycled aggregate concrete. Constr Build Mater 247:118540
Wei Y, Chen P, Cao S, Wang H, Liu Y, Wang Z, Zhao W (2023) Prediction of carbonation depth for concrete containing mineral admixtures based on machine learning. Arab. J. Sci. Eng. 48:1–15
Wei C, Song S (2005) Study on durability of high content fly ash active powder concrete. New Build Mater 9:27–29
Wong HS, Razak HA (2005) Efficiency of calcined kaolin and silica fume as cement replacement material for strength performance. Cem Concr Res 35:696–702
Zeyad AM, Khan AH, Tayeh BA (2020) Durability and strength characteristics of high-strength concrete incorporated with volcanic pumice powder and polypropylene fibers. J Mater Res Technol 9:806–818